Research & Reviews: Journal of Material Sciences

DOI: 10.4172/2321-6212.1000218

e-ISSN: 2321-6212
p-ISSN: 2347-2278

Removal of Iron and Manganese from Aqueous Solution Using Hydroxyapatite Prepared from Cow Bone

Olabiyi OG* and Adekola FA

Department of Industrial Chemistry, University of Ilorin, Ilorin, Nigeria

Research Article

Received: 18/12/2017
Accepted: 27/02/2018
Published: 05/03/2018

***For Correspondence**

Olabiyi OG, Department of Industrial Chemistry, University of Ilorin, Ilorin, Nigeria,
Tel: 08167279809/08067332320.

Email: olabiyiolajumokegbemisola@gmail.com

Keywords: Functionalized hydroxyapatite, Cowbone, Iron, Manganese

ABSTRACT

Functionalized hydroxyapatite was synthesized from cow bone as model adsorbent for the removal of manganese and iron which often occurs as geogenic contaminants in untreated surface and ground water. The adsorption behaviour was studied by batch method. Prepared adsorbent was characterized using Scanning Electron Microscopy (SEM), Energy Dispersive X-ray (EDX), and X-ray Fluorescence. The effect of initial concentration, pH value of aqueous solution, contact time, adsorbent dose and temperature were the parameters used in determining the optimum conditions of the adsorption process. 60 minutes was established to be the adsorption equilibrium time and the equilibrium adsorption experimental data for the metals were establish to suit the Langmuir adsorption isotherms best and the maximum adsorption capacity was 14.68 mg/g and 2.54 mg/g for Mn and Fe respectively. The adsorption kinetics for the adsorbates was defined best by the pseudo second order kinetic model. The adsorption process is endothermic as revealed by the thermodynamic experiment and the reaction is spontaneous as shown from the values of the free energy change. The hydroxyapatite (adsorbent) was applied to typical raw water with 1.52 mg/l and 3.89 mg/l as the initial concentration of manganese and iron respectively and the removal efficiency for Mn and Fe was 91% and 48% respectively. The results shows that the functionalized hydroxyapatite has great prospective for wastewater and water treatment.

INTRODUCTION

The development of effective water treatment methods has been a major challenge for researchers in developing countries and around the world. With growing population, the demand for groundwater has been constantly going up every year. Both groundwater and surface water are tainted by heavy metals which in return generate an environmental hazard due to the fact that metals are not eco-friendly and cause severe contrary effects on human vigor [1]. The existence of manganese and iron compounds in ground and surface water is a severe environmental condition which poses a significant danger to end user and to the natural environment [2]. Due to the reducing conditions of manganese and iron which favors soluble +2 oxidation state, they are found in many ground waters. The management of agricultural wastes is indispensable and a crucial strategy in global waste management. Excess concentration of any type of waste in the environment can become a threat to humans, animals, and vegetation [3]. Some natural biomaterials have been used recently as an adsorbent. The advantages of adsorbents from biomaterials include low operational cost and biodegradability. Rice husk carbon, moringa seeds, fish bones, and various fruit seeds are some of the biomaterials that have been used to remove heavy metals from aqueous solution [4].

Hydroxyapatite (HAP) is a sparingly soluble, stable and inexpensive salt that can be produced through precipitation from calcium phosphate solutions. HAP can remove some heavy metal ions like Cd, Mn, Zn, Co, Fe and Pb ions. Natural HAP is easier to produce and cheaper than synthetic HAP. The adsorption capacity of Natural HAP has been discovered to be almost the same with synthetic HAP. For these reasons, Natural HAP can be a good substitution for synthetic type [5]. Bazargan-Lari et al. [5] in their study used natural hydroxyapatite derieved from bovine femur, tibia, humerus and ulna/chitosan composite for the uptake Zn ions from aqueous solution. In their result they reported that the sorption of zinc ion onto N-HAP/chitosan composite follows the second- order rate kinetics. Values of ΔG° show that the sorption of the Zn (II) ion onto N-HAP/chitosan composite is a favorable spontaneous process. In another related study, Poonam et al investigated the feasibility of the Mg-HAP powder for fluoride removal

e-ISSN: 2321-6212
p-ISSN: 2347-2278
DOI: 10.4172/2321-6212.1000218

from aqueous solution. The Mg-HAP adsorbent developed for fluoride removal from aqueous solution has very good potential for defluoridation with a capacity of 1.4 mg/g and with 10 g/L, Fluoride removal of 92.34% was achieved and equilibrium was reached in 180 min.

The focal objective of this study is to explore the potential use of cow bone, an agricultural waste material as low cost bio-adsorbent for removal of iron and manganese ions from aqueous solution and real raw water from a local dam. The effect of pH, temperature, the effect of initial concentration, adsorbent dose, the effect of contact time on the sorption capacity are some physical–chemical and thermodynamic parameters that were investigated. The data obtained is fitted into some established literature kinetic mathematical models and thermodynamics parameters to determine the kinetics of adsorption.

MATERIALS AND METHOD

Collection of Cow Bones Waste Material

The raw material (Cow bones) collected which is an agro-residue waste material were collected from an abattoir at a local market in Ilorin, Kwara State of Nigeria.

Preparation of Adsorbent

Cow bone was deproteinized externally with 1 (M) HCL solution and finally 1(M) NaOH solution was added for removal of remaining proteins. The cow bones were then thoroughly washed with distilled water and dried in the oven (60-70°C). The dried samples were then calcined in air atmosphere for an hour at different temperatures viz. 1000°C, 1100°C and 1200°C to obtain HAP phase. The calcined bones were grinded to particle size of less than 300 µm and further dried in the oven [6]. The hydroxyapatite obtained was washed with about 140 ml acetone and dried in an oven at 100°C for 4-5 hours. The hydroxyapatite surface was then reacted with 25 g of ethylenediaminetetraacetic acid (EDTA) in 188 ml of mixed ethanol and acetic acid (1:1) solution at 76°C for 16 hours.

Characterization of Adsorbent

Archimedes' principle was the basis used in determining the bulk density of the hydroxyapatite. The equation below was used to determine the bulk density:

$$\text{Bulk density} = \frac{W_2 - W_1}{V}$$

The weight of empty measuring cylinder and the weight of cylinder filled with sample is W_1 and W_2 respectively and the volume of cylinder is V.

The pH of the adsorbent (hydroxyapatite) was determined by weighing 1 g of the adsorbent, boiled for 5 min in a beaker containing 100 ml of distilled water. The solution was diluted to 200 ml with distilled water and cooled at room temperature. A pH meter (model ATPH-6) was used to determine each of the pH and the readings were documented.

The major functional groups present in the adsorbent were determined by Fourier transform infrared spectrometry (FTIR-8400S).

X-ray fluorescence (XRF) spectrometry was used to determine the elemental composition of the adsorbent. For further analysis of the elemental compositions of the sample, energy-dispersive spectroscopy (EDX) was employed (Xflash 6TI30 Bruker). The microstructure and surface morphology and of the functionalized HAP were envisaged by means of scanning electron microscopy (Nova Nano SEM 450).

Batch Adsorption Experiments

The adsorption experiment were conducted using with 20 ml of solutions containing heavy metal ions of preferred concentrations and 0.1 g of FHAP in 100 ml poly vinyl chloride(PVC) bottles at constant temperature of 28 ± 2°C. A mechanical shaker was used to shake the mixture for 5 h and with the use of Whatman filter paper No 1, the mixtures were filtered. The exact concentrations of metal ions in the initial and final solution were determined spectrophotometrically. The equation below was used to calculate the percentage (%) adsorbed.

Where the initial and final concentrations of the metal ions in solution where C_o and C_e respectively.

$$\%\text{Adsorption} = \frac{(Co - Ce)}{Co} X 100$$

Adsorption Isotherm Studies

Langmuir isotherm was used to fit the experimental data [7] and freundlich isotherms [8] were also used in the interpretation of the data. Langmuir equation is represented thus:

$$\frac{C_e}{q_e} = \frac{1}{q_{\max} K_L} + \frac{C_e}{q_{\max}}$$

Where Ce is the equilibrium concentration of adsorbate (mg/l^{-1}) and q_e is the amount of metal adsorbed per gram of the

e-ISSN: 2321-6212
p-ISSN: 2347-2278
DOI: 10.4172/2321-6212.1000218

adsorbent at equilibrium (mg/g). b (l/mg) and q_m (mg/g) are Langmuir constants related rate of adsorption and adsorption capacity respectively. The values of q_m and b were calculated from the slope and intercept of the Langmuir plot of Ce versus Ce/qe [9]. The empirical equation proposed by Freundlich is:

$q=K_fC^{1/n}$

Where the weight adsorbed per unit weight of adsorbent is q and the concentration of the metal solution is C. K_f and n are coefficients. By taking logarithm of the equation and rearranging: log q

$$= \log K_f + \frac{1}{n}\log C$$

The strength of adsorption in the adsorption process is a function of 1/n while the constant K_f is an approximate indicator of adsorption capacity. Linearization of the above equation by making use of mathematical techniques, the values for n and K_f can be obtained [10]. A normal adsorption is an indication that the value for 1/n is below 1. When the partition between the two phases is independent of the concentration then it indicates that the value for n is equal to 1.Subsequently, if 1/n is above 1 it shows cooperative adsorption [11].

Adsorption Kinetics Studies

Lagergren equation which is also known as pseudo-first order rate expression. The experimental data obtained from the experiment at different contact time has been used to test the lagergren equation. It is expressed using this equation.

$$\log(q_e - q) = \log qe - \frac{K_{ad}}{2.303} \times t$$

the slope and intercept of the plot of log (qe - qt) versus t are determined from the values of k_{ad} and qe. k_{ad} (min^{-1}) is the equilibrium rate constant of pseudo- first order adsorption and qe (mg/g) is the mass of metal adsorbed at any time t

To further analyze the adsorption data obtained, pseudo second order model was also used. This model is centered on assumption that adsorption trails a second order mechanism [12].This pseudo second order model is expressed as:

$$\frac{t}{q_t} = \frac{1}{k_2 q_{e^2}} + \frac{1}{q_e} \times t$$

The slope of the plot of t/qt versus t gives the value for q_e and the pseudo-second order rate constant (g/mg/min) is K_2.

Thermodynamic Study

By varying the temperature conditions between 30 and 70°C the thermodynamic parameters were obtained while keeping other variables constant.The variables that were kept constant include metal concentration, pH, contact time and adsorbent dose. The values of the thermodynamic parameters were calculated using the expression below:

$\Delta G° = -RT\ln K_d$

where ΔG° is the standard Gibb's free energy change for the adsorption process (J/mol), R is the universal gas constant (8.314 J/mol/K) while T is the temperature (K). K_d is the distribution coefficient of the adsorbate. The plot of ln K_d versus 1/T gives a straight line with the slope and the intercept giving values of ΔH° and ΔS°.

$\ln K_d = \Delta S/R - \Delta H/RT$

These values could be used to compute ΔG° from the Gibb's relation,

$\Delta G = \Delta H - T\Delta S$

Where K_d is the distribution coefficient of the adsorbate, and it is equal to qe/Ce (l/g). T is the temperature (K), R=8.314 × 10^{-3} kJ K^{-1} mol^{-1}, qe is quantity of metal ion adsorbed (mg/g) and Ce is the equilibrium concentration of metal ion solution (mg/l). ΔG was calculated from the equation at temperature of 303–313 K.

Application of Batch Optimization Conditions for the Removal of Mn and Fe from Untreated Dam Water

The raw Unilorin dam water was collected and thereafter contacted with the prepared FHAP using the optimized condition obtained from the experiment for the adsorption process [13].

RESULTS AND DISCUSSION

The results of the physical chemical properties are summarized in **Table 1**.

Table 1. Physical Chemical properties.

Properties	FHAP
pH	7.5
Bulk density	0.4533
Particle Size	300<θ<250

Research & Reviews: Journal of Material Sciences
e-ISSN: 2321-6212
p-ISSN: 2347-2278
DOI: 10.4172/2321-6212.1000218

X-ray Fluorescence Spectroscopy Analysis

The elemental analysis of the FHAP is summarized in **Table 2**. The result obtained from this analysis reveal that calcium is the major composition of the adsorbent with a percentage composition of 58.44%. While phosphorus constitutes 32.40%.The Ca/P ratio is 1.74/1.81 for HAP/FHAP respectively which is in agreement with the values reported by Lee et al. [14] in his investigation. The data obtained from XRF of FHAP revealed the introduction of N-group onto the hydroxyapatite (HAP).This provides an evidence for the functionalization.

Table 2. X-ray Fluorescence of FHAP.

Elements	Concentration%
Ca	58.44
P	32.4
Mg	0.65
Na	0.73
O	0.93
K	0.42
N	4.42
C	2.01

SEM-EDX Analysis

The SEM images of the functionalized hydroxyapatite (FHAP) at different magnifications are shown in **Figure 1**. The SEM image of the FHAP shows that the adsorbents are in aggregate form which could have been caused by the large surface area. The SEM image of the FHAP at magnification of 50,000 shows that FHAP is in aggregate form. This irregular shape of the particles and also their large sizes might be due to grinding the calcined bone during the production of the hydroxyapatite [13].The morphology of the hydroxyapatite revealed a porous crystalline structure with particle aggregation of various sizes. The occurrence of pores in the hydroxyapatite is very vital as this would affect greatly the uptake of the metal ions and the reactant molecules from the solution.

The results of the SEM-EDX analysis showed the Ca/P ratio of the FHAP investigated in this study varies between 1.46 and 2.01 with an average of 1.80 respectively. The values of Ca/P ratio reported by Lee *et al* during synthesis of hydroxyapatite from cuttlefish bone and phosphoric acid were 1.70 and 1.64 for two different mixing ratios of the calcined cuttlefish bone to phosphoric acid. The Ca/P ratio found in the present investigation agrees with the above values reported by Lee et al. [14]. The energy-dispersive X-ray spectroscopy (EDX) spectrum of FHAP given in **Figure 2** depicts the presence of magnesium, calcium, phosphorus, and oxygen in the structure and Nitrogen.

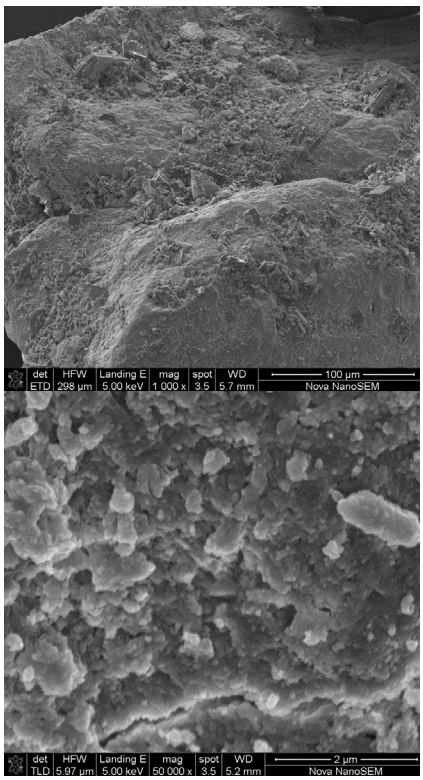

Figure 1. SEM images of FHAP.

Research & Reviews: Journal of Material Sciences
DOI: 10.4172/2321-6212.1000218
e-ISSN: 2321-6212
p-ISSN: 2347-2278

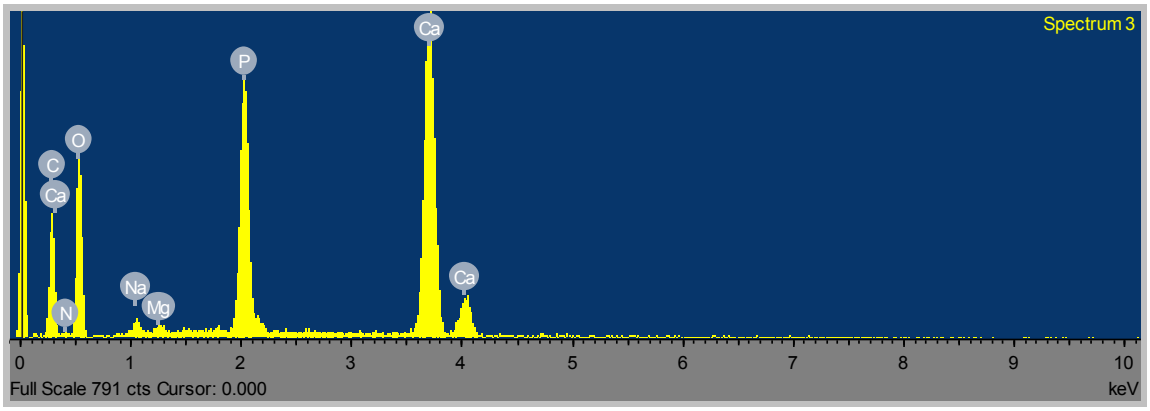

Figure 2. EDX Spectrum of FHAP.

FTIR

The FTIR spectrum of FHAP is presented in **Figure 3**. It shows a series of bands in the mid infrared region ; a strong band at 1033 cm^{-1} another band at 2359 cm^{-1} with a shoulder at 2340 cm^{-1} and also a small sharp band at 609 cm^{-1}. Different types of chemical bonds which are present in various components of hydroxyapatite give characteristic infrared absorption bands. All bands observed in the FTIR of **Figure 2** are associated with the inorganic components of bone which were present in the hydroxyapatite. These bands present can be divided into three main groups which are phosphate, carbonate and hydroxyl groups. From the FTIR spectrum at approximately 1558 cm^{-1}, CO_3^{2-} is observed and is described as substitutes phosphate ion, B type HAP is formed **(Table 3)**. Strong peak at approximately 1033 cm^{-1} denotes PO_4^{3-} and resembles those observed by Raynaud et al. [15]. Medium and peaks of OH^- group were spotted at approximately 1460 cm^{-1}, this correlates with Destainville et al. [16].

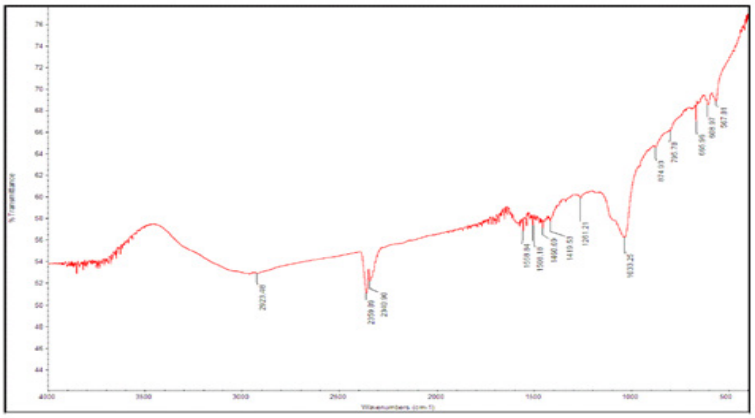

Figure 3. Infrared Spectrum of FHAP.

Table 3. Functional groups of FHAP.

FHAP	Assignment
1033.25	Assymetric stretching vibrations of PO_4^{3-}
1460.69	OH bending vibrations
1558.84	C=O of CO_3^{2-}
2359.89	C≡N
874.93	PO_4^{3-}

Results of Adsorption Studies

Effect of initial concentration: The results obtained are represented in **Figures 4 and 5**.With initial concentration of the metal solution the quantity of metals adsorbed by the adsorbent (FHAP) increased until equilibrium was reached. The highest amount of Fe(II) ion adsorbed using FHAP was 1.80 mg/g and for Mn(II) is 12.02 mg/g. From the amount adsorbed it is evident that FHAP has higher capacity for manganese than iron. As there is an increase in the driving force which arises from the concentration gradient between the bulk solution and the surface of the FHAP, increase in the adsorption capacity was observed. At higher concentrations, the active sites of the adsorbent were surrounded by more Fe(II) and Mn(II) ions and the process of adsorption continues until equilibrium is reached.

Research & Reviews: Journal of Material Sciences
DOI: 10.4172/2321-6212.1000218
e-ISSN: 2321-6212
p-ISSN: 2347-2278

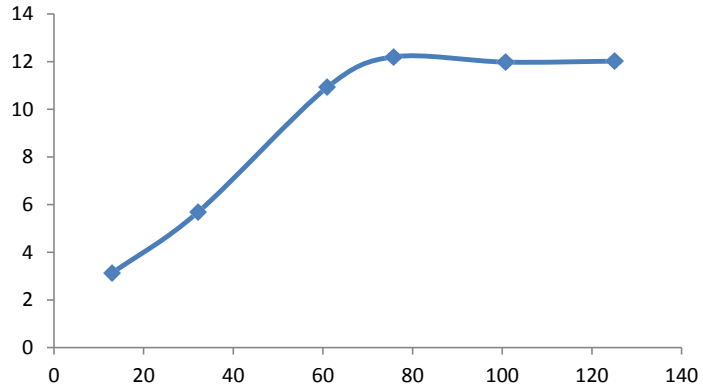

Figure 4. Effect of concentration on the sorption capacity of Mn2+ onto FHAP.

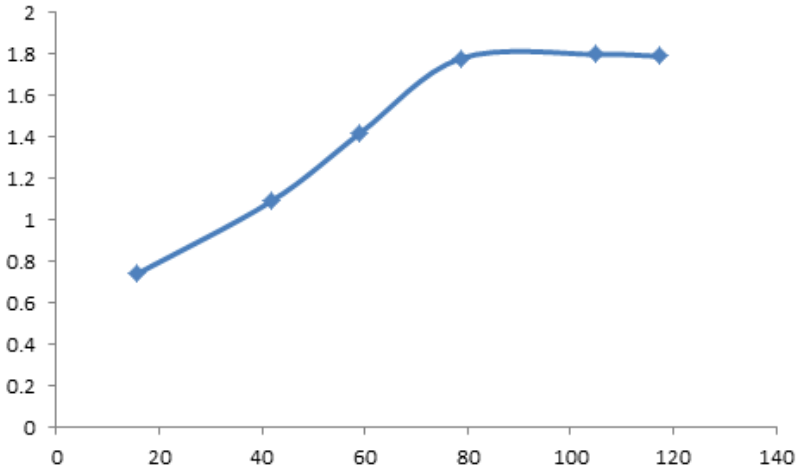

Figure 5. Effect of concentration on the sorption capacity of Fe^{2+} onto FHAP

Effect of pH: It was observed that the percentage removal was increased from 6 to 44% for Fe(II) ions and from 26 to 47% for Mn(II) ions as pH increased from 2-8.The maximum removal for Fe(II) and Mn(II) ions was found to be 44% and 49% at pH 6. This phenomenon may possibly be partly ascribed to the fact that when the pH values increased, the adsorbent surfaces were more negatively charged and thereby attracted to metal ions with positive charges, as a result causing the adsorption onto the FHAP surface [17]. When the maximum adsorption limit is reached, it results into decreasing adsorption efficiency **(Figure 6)**. This decrease in adsorption efficiency may be due to the formation of soluble hydroxylated complexes of the metal ions and the nature of their ionization. Furthermore, at higher pH levels, hydroxide will be formed from Fe(II) and Mn(II) forms and become precipitated. Therefore it cannot be concluded that adsorption or precipitation is responsible for the removal of Fe(II) and Mn(II).

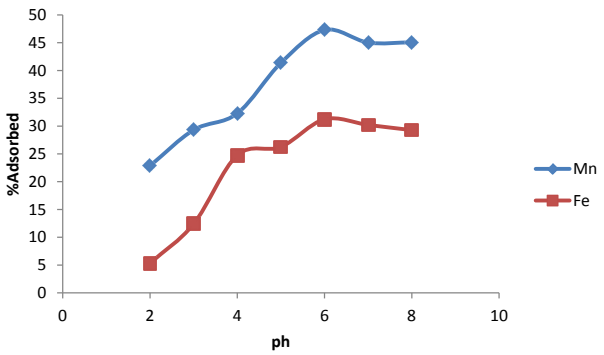

Figure 6. Effect of pH on the sorption capacity of Mn^{2+} and Fe^{2+} onto FHAP.

Research & Reviews: Journal of Material Sciences
e-ISSN: 2321-6212
p-ISSN: 2347-2278
DOI: 10.4172/2321-6212.1000218

Effect of contact time: Contact time effect on the uptake of Fe(II) and Mn(II) onto FHAP was studied and is represented in **Figure 7**. It was observed that the contact time increased up to 60 minutes as the quantity Fe(II) and Mn(II) removed increased. There was no considerable increase after 60 min, the sorption efficiencies for Fe(II) and Mn(II) were 38.97% and 42.10% respectively and 36.65% and 40.71% after 60 min respectively using FHAP. This result may be due to the use of vacant adsorption sites on the adsorbent surface. During the initial stage of sorption, a large number of vacant surface sites were available for adsorption. After a lapse in time, the remaining vacant surface sites were occupied due to repulsive forces between the solute molecules on the adsorbent surface and the bulk phase [18].

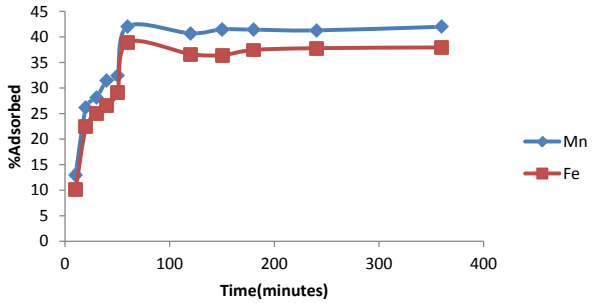

Figure 7. Effect of contact time on the sorption capacity of Mn^{2+} and Fe^{2+} onto FHAP.

Effect of adsorbent dose: The study on the effect of adsorbent dose is indispensable and very expedient in order to find out the most favorable amount of hydroxyapatite necessary for the removal of Fe(II) and Mn(II) ions. **Figure 8** illustrated the effect of the adsorbent dose on the sorption capacity of Fe(II) and Mn(II) ions. The sorption efficiencies of Fe(II) and Mn(II) were found to increase exponentially with the increase of adsorbent dose up to 0.15 g. This may be due to the increase in availability of surface active sites resulting from the increased dose of adsorbent. At higher dosages, 0.15 g and 0.2 g, sorption was almost the same and at maximum. The adsorption site was used up when the adsorption dose reached a certain rate, hence it leads to reduced tendency of the particles to adsorb more ions to its surface [19].

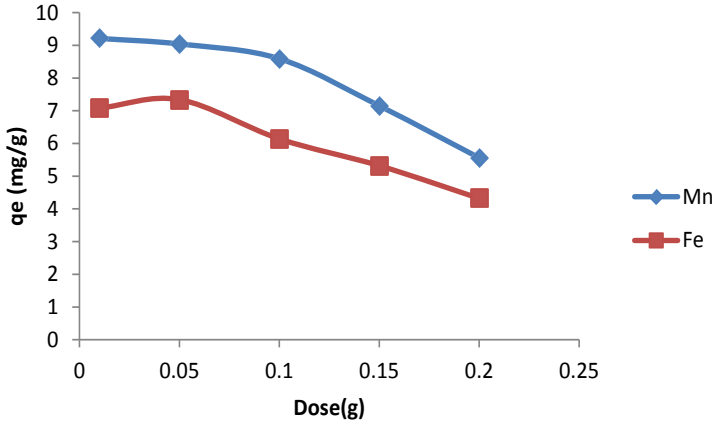

Figure 8. Effect of adsorbent dose on the sorption capacity of Mn^{2+} and Fe^{2+} onto FHAP.

Effect of temperature: As temperature increases, the removal efficiency of both Mn^{2+} and Fe^{2+} increases which was due to increase in number of active sites and the decrease in the thickness of the boundary layer surrounding the FHAP. Furthermore, increasing temperature resulted in an increase in the rate of approach to equilibrium **(Figure 9)**. The decrease in adsorption with the rise of temperature may be due to the formation of the adsorbate– adsorbent complex which becomes unstable resulting in the escape from solid phase to the bulk solution [20].

Research & Reviews: Journal of Material Sciences
DOI: 10.4172/2321-6212.1000218
e-ISSN: 2321-6212
p-ISSN: 2347-2278

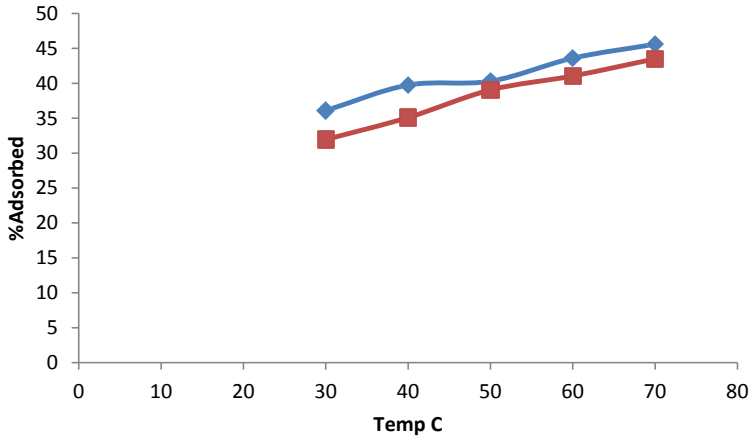

Figure 9. Effect of contact time on the sorption capacity of Mn^{2+} and Fe^{2+} onto FHAP.

Adsorption isotherms: The Freundlich and Langmuir isotherms were used to define the results of the adsorption experiments. Batch adsorption isotherms were carried out on sorption of manganese and iron using FHAP at room temperature. The data obtained from the adsorption isotherm are represented in **Figures 10-13**.

The results of Langmuir isotherm best fitted adsorption Mn(II) on FHAP with correlation coefficient R^2 0.98 and reasonably fitted the adsorption for Fe(II) with correlation coefficient R^2 0.96. The plots of Ce versus Ce/qe for Mn(II) and Fe(II) are shown in **Figures 10 and 12. Table 4** also shows the linear isotherm parameters (q_m, b) and the correlation coefficient. Maximum sorption capacity, qm of Mn(II) is 12.87 mg/g which is larger than that of Fe(II) of 2.39 mg/g, this shows that the FHAP has greater ability to adsorb Mn(II) than Fe(II). The good agreement of Langmuir isotherm with the adsorption may be due to homogenous distribution of active sites on the adsorbent since the Langmuir equation assumes that the surface is homogenous [21-26].

The freundlich isotherm also fairly describe the adsorption process with correlation coefficient R^2 0.89 for Mn(II) and 0.66 for Fe(II). The values for k_f and 1/n were determined from the slope and intercept of the plot of log Ce versus log qe. The freundlich constant n is (3.50, 2.23) for Mn(II) and Fe(II) respectively.Since the constant lies between 1 and 10,it shows that the adsorption is favorable.

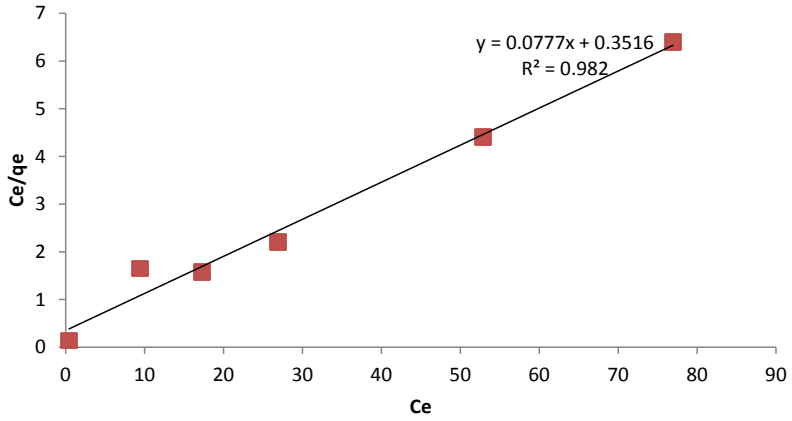

Figure 10. Langmuir plot for sorption of Mn(II) ions on FHAP.

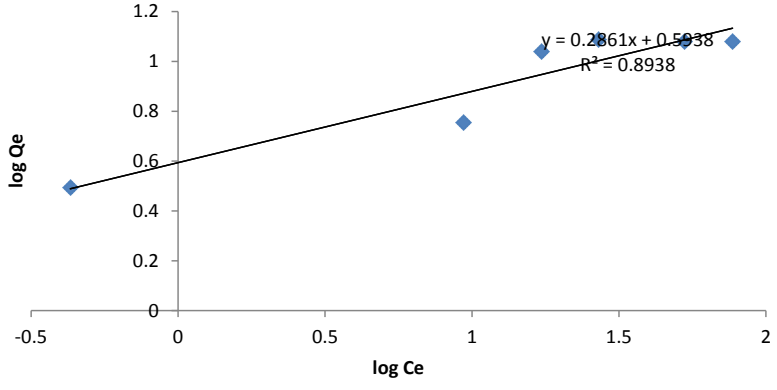

Figure 11. Freundlich plot for sorption of Mn(II) ions on FHAP.

Research & Reviews: Journal of Material Sciences
DOI: 10.4172/2321-6212.1000218
e-ISSN: 2321-6212
p-ISSN: 2347-2278

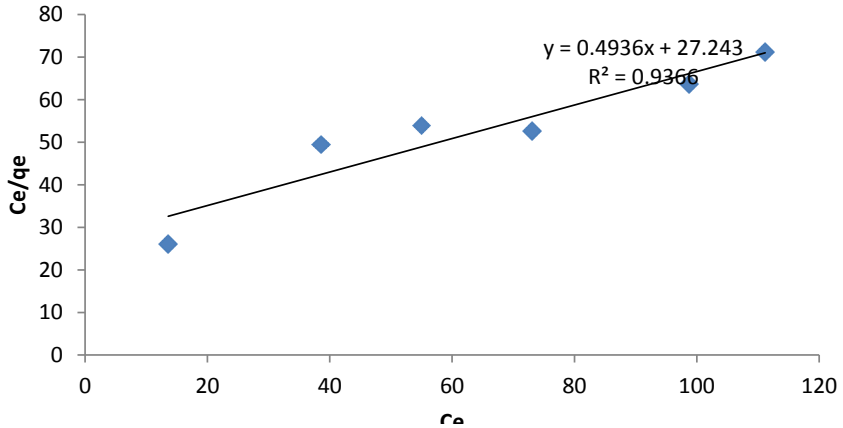

Figure 12. Langmuir plot for the sorption of Fe(II) ions on FHAP.

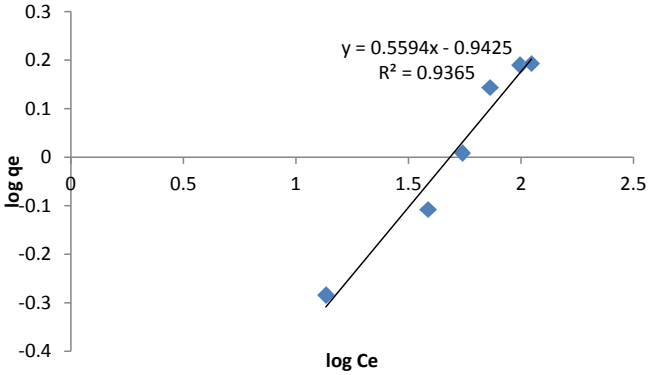

Figure 13. Freundlich plot for the sorption of Fe(II) ions on FHAP.

Thermodynamic Studies

The data obtained for the thermodynamics parameters are presented in **Table 4**. Some thermodynamic parameters such as enthalpy change (ΔH), entropy change (ΔS) and Gibbs free energy change (ΔG) could be determined during adsorption studies using the data obtained from temperature change. The effect of temperature on the sorption of iron and manganese ions onto FHAP is shown in **Figures 14 and 15**. There was increase in the removal efficiency of both Fe(II) and Mn(II) as the temperature increases which was as a result of increase in the number of active sites surrounding the adsorbent. At initial metal concentration of 20 ppm and pH 6 The free energy change values obtained for the adsorption of Mn(II) and Fe(II) at 313 K were -1565.56 and -414.56 kJ mol^{-1} respectively [27-31].

Table 4. Thermodynamics parameters for Mn(II) and Fe(II) ions.

Metals	Enthalpy change ΔH(KJ/mol)	Entropy change ΔS(KJ/mol/k)	Gibbs free energy change ΔG($Jmol^{-1}$)
Mn(II)	9383.18	34.98	-1565.56
Fe(II)	8183.55	27.47	-414.56

Research & Reviews: Journal of Material Sciences
DOI: 10.4172/2321-6212.1000218
e-ISSN: 2321-6212
p-ISSN: 2347-2278

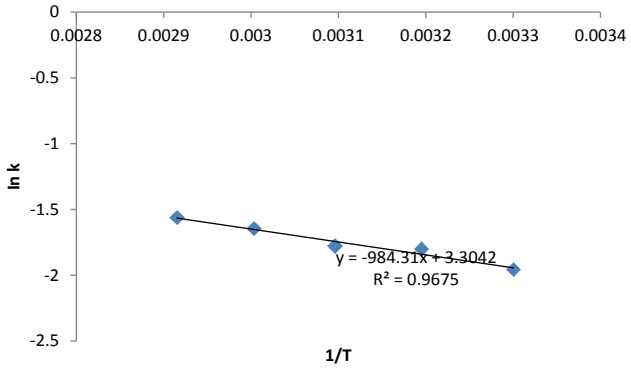

Figure 14. A plot of InKd against 1/T for sorption of Fe^{2+} onto FHAP.

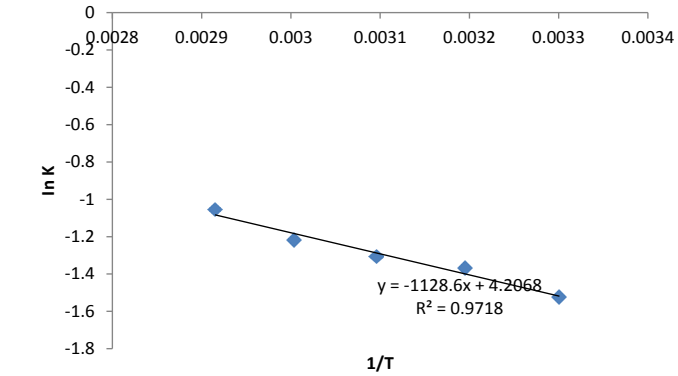

Figure 15. A plot of InKd against 1/T for sorption of Mn^{2+} onto FHAP.

Adsorption Kinetics

Adsorption kinetics, which is one of the important characteristics defining the adsorption efficiency of the surface of the adsorbent, describes the solute uptake rate. The results of the kinetic studies of adsorption of Mn^{2+} onto HAP/FHAP are shown in **Figures 16 and 17** while the parameters are shown in **Table 5**. The kinetic data of Mn(II) and Fe(II) interactions with FHAP were, therefore, tested with different models such as pseudo-first order and pseudo-second order. The adsorption data fit best pseudo second order [32-36]. The adsorption kinetic data for the various models are presented in **Figures 16 and 17**.

A plot of t versus t/qt was used to determine the correlation coefficient and rate constants. The rate constant was 8.1×10^{-3} and 7.3×10^{-3} g/mg/min for Mn(II) and Fe(II) respectively.

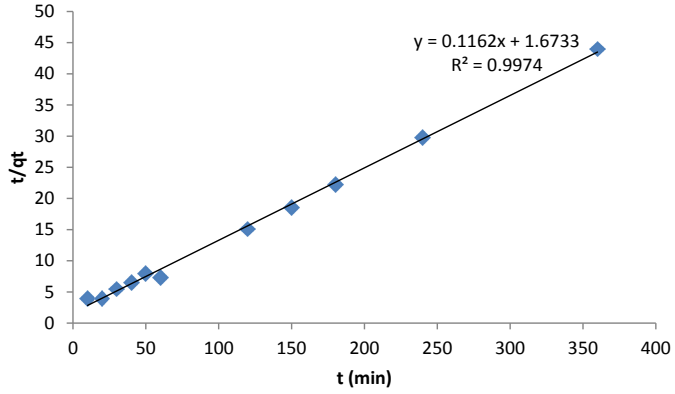

Figure 16. Pseudo-second order kinetics for sorption of FHAP on Mn(II) ions.

Research & Reviews: Journal of Material Sciences
DOI: 10.4172/2321-6212.1000218
e-ISSN: 2321-6212
p-ISSN: 2347-2278

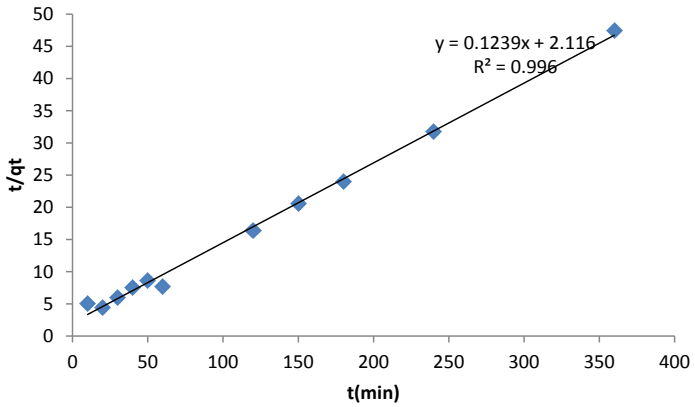

Figure 17. Pseudo-second order kinetics for sorption of FHAP on Fe(II) ions.

Table 5. Kinetics parameters for the sorption of Mn(II) and Fe(II) ions

Metals	qe	K_2	R^2
Mn(II)	8.61	0.0081	0.998
Fe(II)	8.07	0.0073	0.997

Comparison of Adsorption Capacities of prepared hydroxyapatite

The sorption capacities of the prepared adsorbent (hydroxyapatite) for the sorption of manganese ions and iron ions obtained from this research work were related with that of other adsorbents that has been stated by past researchers and the comparison is abridged in **Table 6**. It showed to be an improved adsorbent for the sorption of Mn(II) ion and Fe(II) ion from aqueous solution than some of the adsorbents described in prior works [37-41].

Table 6. Comparison of maximum adsorption capacities of different adsorbents for Mn^{2+} and Fe^2

Mn(II)	Adsorbent	Adsorption Capacity (mg/g)	Reference
	Rice husk ash	3.17	[42]
	Clay	7.79	[43]
	Bovine bone	29.56	[44]
	FHAP	12.87	Present work
Fe(II)	Rice husk ash	66.66	[42]
	Pine bark wastes	2.03	[45]
	FHAP	2.39	Present work

Removal of Fe(II) and Mn(II) from Unilorin Dam Water

The untreated dam water (Unilorin) was collected and was contacted with the prepared FHAP using the optimized condition for the adsorption process. The percentage removal of Fe(II) and Mn(II) were 48% and 91% respectively as shown in **Figure 18**. The final concentration of manganese from the result after adsorption which was 0.134 mg/l shows that it is safe for drinking according to the BIS guideline value given by Nigerian Standard for Drinking Water Quality (NIS 554:2007/SON). But in the case of final concentration of iron, the final concentration was 2.012 mg/l which is still not safe for drinking. Therefore, there is need for undergoing another cycle of adsorption by contacting with the hydroxyapatite adsorbent [46-51].

e-ISSN: 2321-6212
p-ISSN: 2347-2278
DOI: 10.4172/2321-6212.1000218

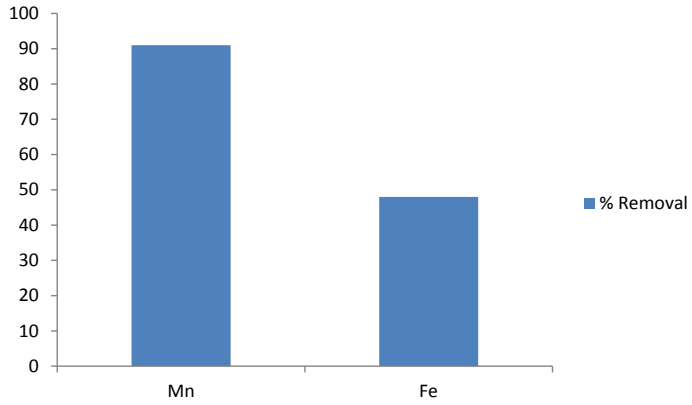

Figure 18. Removal of Fe(II) and Mn(II) from untreated Dam Water using FHAP.

CONCLUSION

It can be concluded from this study that the functionalized hydroxyapatite prepared from cow bone is an effective adsorbent for the removal of Fe(II) and Mn(II) ions from aqueous solution. The amounts of Fe(II) and Mn(II) ions adsorbed were found to hinge on the amount of the adsorbent used, pH, contact time of adsorption, temperature and initial concentrations of the adsorbent. Langmuir isotherm described all the adsorption processes better than all other isotherm models that were used in the study and Pseudo second order kinetics was found to described the kinetics of the adsorption process. The values of the Gibbs free energy got from the thermodynamics study further shows that all the adsorption processes are feasible and spontaneous. The adsorbent used in the study proved that it is a better adsorbent for Mn(II) since it has the highest value of adsorption.

REFERENCES

1. Spellman FR. Handbook for waterworks operator certification, Vol 2. Technomic Publishing Company Inc, Lancaster 2001;6:81-83.
2. Adekola FA, et al. Thermodynamic and kinetic studies of biosorption of iron and manganese from aqueous medium using rice husk ash. Appl Water Sci 2014;6:319-330.
3. Abdulrahman I, et al. From Garbage to Biomaterials : An Overview on Egg Shell Based Hydroxyapatite. J Mater 2014;6:234-240.
4. Jahn SAA. Using Moringa Oleifera seeds as coagulant developing countries. JAM Water Works Assoc 1988;6:43-50.
5. Bazargan-Lari R, et al. Removal of Cu(II) ions from aqueous solutions by low-cost natural hydroxyapatite/chitosan composite: Equilibrium, kinetic and thermodynamic studies. J Taiwan Inst Chem Eng 2014;45:1642-1648.
6. Mondal S, et al. Processing of natural resourced hydroxyapatite ceramics from fish scale. Adv Appl Ceram: Struct Funct Bioceram 2010;109:234-239.
7. Vermeulan, et al. Fundamental. Ind Eng Chem 1966;5:212-223.
8. Hutson ND and Yang RT. Theoretical basis for the Dubinin-Radushkevitch (DR) adsorption isotherm equation. Adsorption. 1997;3:189-195.
9. Langmuir I. The evaporation of small spheres. Physical Rev 1918;12:368.
10. Voudrias E, et al. Sorption - Desorption Isotherms of Dyes from Aqueous Solutions and Wastewaters with Different Sorbent Materials. Global Nest the Int J 2002;4:75-83.
11. Mohan SV and Karthikeyan J. Removal of lignin and tannin colour from aqueous solution by adsorption onto activated charcoal. Environ Pollut 1997;97:183-187.
12. Ho YS and McKay G. Pseudo-second-order model for sorption processes. Process Biochem 1999;34:451-465.
13. Javidi M, et al. Characterisation of natural hydroxyapatite extracted from bovine cortical bone ash. J Ceram Process Res 2009;10:129-138.
14. Lee CK, et al. The removal of heavy metals using hydroxyapatite. Environ Eng Res 2005;10:205-212.
15. Raynaud, et al. Calcium phosphate apatites with variable Ca/P atomic ratio I. Synthesis, characterisation and thermal stability of powders. Biomaterials 2002;23:1065-1072.
16. Destainville, et al. Synthesis, characterization and thermal behavior of apatitic tricalcium phosphate. Mater Chem Phys 2003;80:269-277.

e-ISSN: 2321-6212
p-ISSN: 2347-2278
DOI: 10.4172/2321-6212.1000218

17. Taffarel SR and Rubio J. On the removal of Mn2+ ions by adsorption onto natural and activated Chilean zeolites. Miner Eng 2009;22:336-343.

18. Wongjunda and Saueprasearsit. Biosorption of chromium (VI) using rice husk ash and modified rice husk ash. Environ Res J 2010;43:244-250.

19. Onundi, et al. Adsorption of copper, nickel and lead ions from synthetic semiconductor industrial wastewater by palm shell activated carbon. Int J Environ Sci Technol 2010;7:751-758.

20. Gupta N, et al. Adsorption of Cobalt(II) from aqueous solution onto hydroxyapatite/zeolite composite. Adv Mater Lett 2011;2:309-312.

21. Admassu W and Breese T. Feasibility of using natural fishbone apatite as a substitute for hydroxyapatite in remediating aqueous heavy metals. J Hazard Mater 1999;69:187-196.

22. Alexandroaei M, et al. The removal of the Pb^{2+} ions from solutions by a hydroxyapatite nanomaterial. Revista de Chimie 2013;64:1100-1103.

23. APHA American Public Health Association. Standards method for the examination of water and wastewater 1995.

24. APHA-American Public Health Association. Standard methods for examination of water and wastewater. Method 5220C, 1999.

25. Babel S and Kurniawan TA. Low-cost adsorbents for heavy metals uptake from contaminated water: a review. J Hazard Mater 2003;97:219-243.

26. Choi S and Jeong Y. The removal of heavy metals in aqueous solution by hydroxyapatite/cellulose composite. Fibers Polym 2008;9:267-270.

27. Conca JL and Wright J. An apatite II permeable reactive barrier to remediate groundwater containing Zn, Pb and Cd. Appl Geochem 2006;21:2187-2200.

28. Connell DW and Miller GJ. Chemistry and Ecotoxicology of Pollution. J Mater 1984;7:344-362.

29. Eletta OA. Physico–Chemical Characterization, Speciation and interaction studies of some pollutants in the water and sediments of Asa River, Ilorin. Nigeria. Ph.D thesis. University of Ilorin, Ilorin. Nigeria 2004;235.

30. Fetter CW. Sorption description isotherms of dyes from aqueous solutions and waste waters with different sorbent materials, global nest. Appl Hydrogeol 1988;4:75-83.

31. Harrison. Ecology and Quality of water resources. New York Basic books 1992.

32. Jang SH, et al. Removal of lead ions in aqueous solution by hydroxyapatite/polyurethane composite foams. J Hazard Mater 2008;152:1285-1292.

33. Jang H and Kang SH. Phosphorus removal using cow bone in hydroxyapatite crystallization. Water Res 2002;36:1324-1330.

34. Kharbanda A and Prasanna K. Extraction of nutrients from dairy wastewater in the form of map (magnesium ammonium phosphate) and hap (hydroxyapatite). J Mater 2016;9:215-221.

35. Kim WG, et al. Removal of Cu(II) with hydroxyapatite (animal bone) as an inorganic ion exchanger. Desalination Water 2009;9:253-264.

36. Lakherwal D. Adsorption of Heavy Metals: A Review. Int J Environ Res Develop 2014;4: 2249-3131.

37. Filipenkovs V, et al. Mechanical properties of cattle bone tissue and natural hydroxyapatite. Scientific Proceedings of Riga Technical University, Series 1: Mater Sci Appl Chem 2012;25:2012.

38. Mondal P and George S. Removal of Fluoride from Drinking Water Using Novel Adsorbent Magnesia-Hydroxyapatite. Water Air Soil Pollut 2015;226:241.

39. Sri Asliza M, et al. Study the Properties of Dense Hydroxyapatite - Extract From Cow Bone. J Nucl Relat Technol 2009;6:175-182.

40. Tebbutt THY. Principles of water quality control. Butterworth Heinemann, UK 2002;8:153-183.

41. Temkin M and Pyzhev JAV. Kinetics of ammonia synthesis on promoted iron catalysts. Acta Physiochem 1940;12:217-222.

42. Adekola FA and Eletta OAA. A study of heavy metal pollution of Asa River, Ilorin. Nigeria; trace metal monitoring and geochemistry. Environ Monit Assess 2007; 125:157-163.

43. Eba F, et al. Evaluation of the absorption capacity of the natural clay from Bikougou (Gabon) to remove Mn (II) from aqueous solution. Int J Eng Sci Technol 2010;2:5001-5016.

e-ISSN: 2321-6212
p-ISSN: 2347-2278
DOI: 10.4172/2321-6212.1000218

44. Juan et al. Optimal microvessel density from composite graft of autogenous maxillary cortical bone and anorganic bovine bone in sinus augmentation: influence of clinical variables. Clin Oral Impl Res 2010;221-227.

45. Acemio et al. Copper (II) adsorption from aqueous solution by herbaceous peat. J Colloid Interf Sci 2004;269:303-309.

46. Ungureanu DN, et al. Synthesis and Characterization of Hydroxyapatite Nanopowders by Chemical Precipitation. Recent Res Commun, Autom, Signal Process, Nanotechnol, Astron Nuclear Phys 2011;296-301.

47. Vasanthavigar M, et al. Application of water quality index for groundwater quality assessment. Environ Monit Assess 2010;171:595-609.

48. Vega ED, et al. Removal of oxovanadium(IV) from aqueous solutions by using commercial crystalline calcium hydroxyapatite. Water Res 2003;37:1776-1782.

49. Wasim M, et al. Synthesis and Characterization of Hydroxyapatite Powder from Natural Bovine Bone. J Bioimmetics Biomater, Tissue Eng 2014;19:35-42.

50. Yidana SM and Yidana A. Assessing water quality using water quality index and multivariate analysis. Environ Sci 2009;59:1461-1473.

51. Zelichenko EA, et al. Investigation of the Properties of Hydroxyapatite Extracted from the Bone Tissue of Agricultural Animals. Chem Sustain Develop 2012;20:491-496.